Development 122, 1281-1289 (1996)
Printed in Great Britain © The Company of Biologists Limited 1996
DEV3317

Confocal microscopy analysis of living *Xenopus* eggs and the mechanism of cortical rotation

Carolyn A. Larabell[1,*], Brian A. Rowning[2], Jonathan Wells[2], Mike Wu[2] and John C. Gerhart[2]

[1]Lawrence Berkeley Laboratory and [2]Department of Molecular and Cell Biology, University of California at Berkeley, Berkeley, CA 94720, USA

*Author for correspondence (e-mail: larabell@lbl.gov)

SUMMARY

The dorsoventral body axis in amphibian embryos is established by a rotation of the outer cortex relative to the inner cytoplasmic core. This cortical rotation depends on microtubules and is correlated with a parallel array of microtubules just inside the vegetal cortex. Since the parallel array moves with the inner cytoplasm and most of its microtubules are oriented with their plus ends facing the direction of cortical movement, it has been suggested that plus end-directed motor molecules attached to the cortex drive the rotation by moving along microtubules of the parallel array. Using an inverted confocal microscope to examine living eggs, however, we found that rotation movements precede the formation of a detectable parallel array at the vegetal pole, that the parallel array consists of multiple layers of microtubules at depths ranging from 4 to 8 μm inside the plasma membrane and that the velocity of rotation in immobilized eggs increases with depth in this region. These findings suggest that (1) early cytoplasmic movements are due to something other than the fully formed parallel array and (2) the motor molecules responsible for the bulk of the rotation movement are not restricted to a monolayer at the subcortical interface but may be distributed throughout the parallel array, perhaps causing microtubules to slide along other microtubules by a mechanism similar to that seen in cilia and eukaryotic flagella.

Key words: cortical rotation, *Xenopus*, microtubule, confocal microscopy

INTRODUCTION

In many animal species, normal embryonic development depends on the proper positioning of cytoplasmic constituents by the egg cytoskeleton. *Drosophila* oocytes utilize microtubules to transport and localize morphogenetic determinants (Theurkauf et al., 1993; Theurkauf, 1994). In ascidians, fertilized eggs undergo a microfilament-mediated cytoplasmic contraction and a microtubule-dependent cytoplasmic rotation which localize morphogenetic determinants in a yellow crescent (Sardet et al., 1989; Sawada and Schatten, 1989). Normal development in amphibians involves a microtubule-dependent rotation of the egg cortex approximately 30° relative to the inner cytoplasm during the first cell cycle (Ancel and Vintemberger, 1948; Manes et al., 1978; Ubbels et al., 1983; Vincent et al., 1986, 1987).

The direction of cortical rotation in fertilized frog eggs is usually (though not always) correlated with the sperm entry point (Ancel and Vintemberger, 1948; Black and Gerhart, 1985; Elinson, 1975; Kirschner et al., 1980). Since the sperm forms a large aster composed of microtubules after entering the egg, it has been suggested that astral microtubules may orient or even drive the rotation (Gerhart et al., 1981; Ubbels et al., 1983). But artificially activated eggs and isolated vegetal fragments (which lack sperm asters entirely) can also undergo cortical rotation (Ancel and Vintemberger, 1948; Gerhart et al., 1986; Vincent et al., 1987), so it appears that astral microtubules are not necessary for rotation even though, when present, they may help to orient it.

In 1988, Elinson and Rowning described an array of parallel microtubules just inside the vegetal cortex of rotating frog eggs. This subcortical array appears at the beginning of (and disappears at the end of) the rotation period, is invariably oriented parallel to the direction of movement and is found in both activated and fertilized eggs (Elinson and Rowning, 1988), as well as in isolated vegetal fragments (Elinson and Palecek, 1993). These correlations suggest that it is the microtubules in the subcortical parallel array, rather than those in the sperm aster array, that are necessary for rotation.

Houliston and Elinson (1991a) subsequently demonstrated that most microtubules in the parallel array are oriented with their plus ends facing the future dorsal side of the embryo, and Rowning (1993) and Houliston (1994) observed that the subcortical array moves with the inner core of cytoplasm rather than the outer cortex. Since the cortex moves (relative to the inner core of cytoplasm) toward the future dorsal side, these observations suggest that rotation may be driven by plus end-directed motor molecules which are anchored to the cortex and move along microtubules of the parallel array. Consistent with this suggestion, antibodies against the kinesin-related protein

Eg5 label microtubules in the subcortical array (Houliston et al., 1994).

In order to characterize more precisely the role of the parallel array in cortical rotation, we used confocal microscopy to obtain serial optical sections of the outermost 15 μm of the vegetal pole region of fertilized and activated *Xenopus* eggs (approximately 1200-1300 μm in diameter) during the first cell cycle. By staining live eggs with Nile Red, we were able to follow the movements of yolk platelets near the vegetal pole and, by injecting fluorescently labeled tubulin, we were able to monitor microtubule polymerization and parallel array formation. These methods enabled us to study the kinematics of cortical rotation at a higher resolution than previously obtained.

MATERIALS AND METHODS

Eggs and embryos

Adult *Xenopus laevis* were raised in the laboratory and fed trout chow (Purina) twice a week. Ovulation was induced by injecting 800 units of human chorionic gonadotropin (Sigma) into the dorsal lymph sac of each frog. Approximately 12 hours later, eggs were stripped into a dry Petri dish and fertilized by overlaying them with approximately one eighth of a minced testis suspended in 1-2 ml of 1/3 strength modified amphibian Ringer's solution (MR; 100% MR: 100 mM NaCl, 2 mM KCl, 1 mM $MgCl_2$, 2 mM $CaCl_2$, 50 mg/ml Gentamycin and 5 mM Hepes, adjusted to pH 7.2 with NaOH). Fertilization was allowed to proceed for 6-8 minutes before dejellying eggs with 2.5% cysteine hydrochloride in 1/3 MR, adjusted to pH 8.0 with NaOH. Eggs were then rinsed 3-5 times with fresh 1/3 MR. Alternatively, some eggs were activated rather than fertilized, by placing them in a 3×3×1 cm deep plexiglass chamber containing 100% MR and applying 12 volts DC for 1 second (from a Heathkit Model IP17 power supply). Activated eggs were promptly removed from the chamber, rinsed in 1/3 MR and dejellied as described above.

Confocal microscopy of live eggs

Visualization of cytoplasmic constituents using vital dyes

Viewing dishes were made by replacing the bottom of a plastic Petri dish with a no. 1 glass coverslip (Baxter), pouring in a thin layer of low gelling-temperature agarose (Sigma) in 1/3 MR and using 1.6 mm-diameter steel balls to produce specimen wells in the molten agarose. After the agarose had cooled, the steel balls were removed and the dish was filled with a solution of 5% Ficoll (Sigma) in 1/3 MR. Immediately after being fertilized and dejellied, eggs were stained for 5 minutes in a solution of 1 μg/ml Nile Red (Polysciences, Warrington, PA (Greenspan et al., 1985)) in 1/3 MR, then removed and rinsed 2-3 times in fresh 1/3 MR before placing them in wells in the viewing dish. Alternatively, some eggs were placed in a viewing dish lacking agarose wells but coated with 0.1% poly-L-lysine to facilitate adhesion of eggs to the coverslip.

The images shown in Figs 1-4 and 6-8 were made with an MRC-1000 laser scanning confocal microscope (Bio-Rad Microsciences, Cambridge, MA) equipped with an inverted Nikon Diaphot 200 microscope and a 60× PlanApo oil immersion objective lens (1.4 numerical aperture). The images shown in Figs 5 and 9 were made with a Leica TCS 4D confocal scanner equipped with an inverted Leitz DM IRB microscope with a 40× objective (Leica Lasertechnik, Heidelberg, Germany). Consecutive z-series were collected over periods ranging from 10 to 30 minutes, as eggs underwent cortical rotation. Using Molecular Dynamics ImageSpace 3.10 software on a Silicon Graphics Indigo workstation, computerized 'movies' were made from the confocal images to facilitate observation of organelle movements; in many cases, the same organelle could be tracked through seven or eight successive images (each 1-2 minutes apart). Velocities were calculated by averaging distance measurements of at least three (and sometimes as many as nine) yolk platelets which could be followed through at least two successive images and then dividing by the exact time between the images.

Visualization of microtubules

To visualize microtubules as well as organelle movements, we injected fluorescein-labeled tubulin (10 mg/ml; Cytoskeleton, Denver, CO) into some eggs, rhodamine-labeled tubulin (10 mg/ml; gift of Tim Mitchison, University of California, San Francisco, CA) into others and caged fluorescein-labeled tubulin (10 mg/ml C2CF; also a gift of Tim Mitchison [Sawin and Mitchison, 1991]) into still others. In each case, labeled tubulin was kept on ice until immediately before injecting to prevent it from polymerizing prematurely. Using a glass injection needle (tip diameter 5 μm), approximately 20 nl was injected into the center of each fertilized egg during incubation in Nile Red solution. Caged tubulin was photoactivated with a 50 μm diameter mercury-arc beam using a Hoechst filter. Injected specimens were examined by confocal microscopy using the fluorescein and rhodamine channels fitted with the appropriate filters, either one at a time or both simultaneously.

Examination of fixed eggs

To verify that the depth differences that we observed were not due to some distortion produced by the apparatus, we fixed five Nile Red-stained eggs by placing them for 4-5 hours in microtubule assembly buffer (80 mM potassium Pipes pH 6.8, 5 mM EGTA, 1 mM $MgCl_2$) containing 3.7% formaldehyde, 0.25% glutaraldehyde and 0.2% Triton X-100 (Gard, 1993; Gard and Kropf, 1993). Subsequently, after obtaining a z-series of images with each egg, we manually moved the microscope stage approximately 200 μm and obtained a second z-series in which the same organelles were visible on the opposite side of the computer screen. Distance measurements at each depth were then made as described above.

RESULTS

Cortical rotation begins by 0.3 normalized time

Fertilized, dejellied eggs were incubated in Nile Red to label the yolk platelets and then placed in Ficoll and agarose wells to immobilize them for confocal microscopy. Since the egg surface was immobilized, cortical rotation was observed as a movement of the inner cytoplasm toward the sperm entry site (Vincent et al., 1986). Serial optical sections of the vegetal pole region were collected starting as early as 0.20 normalized time (NT; normalized time of the first cell cycle, in which 0.0 = fertilization and 1.0 = first cleavage) and stopping when movement was no longer detected, usually by 0.90 NT. The first section of each series was collected at the outermost region of labeled yolk platelets (closest to the cell surface) and each successive section was collected 1 μm deeper in the egg. For analysis, we retrieved all sections collected from a single optical plane over time, as described in the Materials and Methods. We analyzed images only from those eggs that subsequently developed into normal, swimming tadpoles.

The resolution provided by the confocal microscope allowed visualization of individual dye-labeled yolk platelets at precise depths during rotation. Previous studies used fluorescence microscopy to observe movements of large spots consisting of many dye-labeled platelets (Vincent et al., 1986) but, with standard epi-fluorescence techniques, the light scattering due to the thickness of the egg prevents precise resolution of vari-

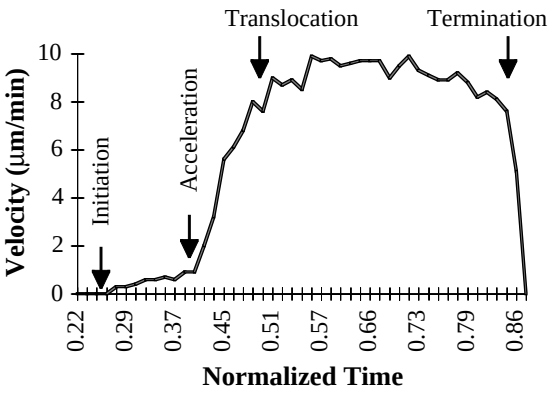

Fig. 1. Velocity of yolk platelets throughout cortical rotation, in a plane perpendicular to the animal-vegetal axis and 8 μm inside the plasma membrane, at the vegetal pole of a fertilized, immobilized egg. Four phases of cortical rotation can be distinguished: (1) initiation - onset of slow movements between 0.28 and 0.40 NT; (2) acceleration - increase of velocity between 0.40 and 0.50 NT; (3) translocation - continuation of maximal velocity between 0.50 and 0.85 NT, as the cortex undergoes the bulk of its displacement relative to the inner cytoplasmic core; and (4) termination - rapid deceleration after 0.85 NT, sometimes followed by slight reversal of direction.

ations of movement with depth. Fig. 1 shows the average velocity of yolk platelets throughout the rotation period, in a plane approximately 8 μm from the vegetal cell surface.

By observing single yolk platelets, we were able to detect small displacements in the direction of cortical rotation earlier than previously noted. Before 0.28 NT, virtually no movement of platelets is detected; even Brownian motion is minimal, presumably due to the tight packing of cytoplasmic organelles (Fig. 2A). At 0.28 NT, individual yolk platelets commence small jostling movements (<0.3 μm), with no unified direction. Within 1 or 2 minutes, however, these movements become oriented in one direction (Fig. 2B). Once this oriented movement begins, the direction of cortical rotation is set; in all the eggs we examined (n=30), subsequent movement deviated less than 20˚ from this initial direction.

Slow movements (<1 μm/minute) continue for several more minutes, then a rapid acceleration occurs between 0.40 and 0.45 NT; this is the time that previous investigators had reported to be the beginning of rotation (Elinson and Rowning, 1988; Vincent et al., 1986). Acceleration continues until about 0.50 NT (Fig. 3), when rotation attains its maximal velocity (of the order of 10 μm/minute). At the 8 μm depth shown in Fig. 1, the velocity then remains relatively constant until after 0.85 NT, at which time a rapid deceleration is observed. In fact, a slight reversal of direction is often noticeable just before first cleavage. Based on these results, we find it convenient to distinguish four phases in cortical rotation:

(1) *initiation* - onset of slow movements between 0.28 and 0.40 NT;

(2) *acceleration* - increase of velocity between 0.40 and 0.50 NT;

(3) *translocation* - continuation of maximal velocity between 0.50 and 0.85 NT, as the cortex undergoes approximately 75% (≈300 μm) of its total displacement relative to the inner cytoplasmic core;

(4) *termination* - rapid deceleration after 0.85 NT, sometimes followed by slight reversal of direction.

At the beginning of the initiation phase, yolk platelets in the vegetal hemisphere are very densely packed (Fig. 2A). By the end of the acceleration phase, however, platelets are separated by sinuous, non-fluorescent channels (Fig. 3). These channels form at the same normalized time that previous investigators have reported the earliest appearance of the parallel array (0.45-0.50 NT) and their roughly parallel pattern resembles that of fluorescently labeled microtubules seen in fixed eggs (Elinson and Rowning, 1988; Schroeder and Gard, 1992). To confirm our suspicion that these channels represent microtubule bundles, we microinjected fluorescein-labeled tubulin into fertilized eggs that were also stained with Nile Red. Microtubule polymerization and yolk platelet displacement were then monitored simultaneously and microtubules were seen filling the channels between the yolk platelets (Fig. 4). Subsequently, we monitored parallel array formation in many eggs without observing labeled microtubules directly, relying instead on the 'negatively stained' microtubule channels outlined by Nile Red-labeled yolk platelets.

The channels often exhibit easily recognizable characteristics, such as the 'X' in Fig. 3, which can be followed for extended periods of time. Individual yolk platelets appear to be associated with specific sites on these microtubule bundles (arrow, Fig. 3) and are seen in that same position in subsequent images. By observing the movements of these channels and their associated yolk platelets, we confirmed earlier reports by Rowning (1993) and Houliston (1994) that the parallel array of microtubules moves with the cytoplasm rather than the cortex during rotation.

Rotation velocity increases with depth from 4 to 8 μm

To study the kinematics of cortical rotation, we measured the velocity of yolk platelets and microtubule bundles at various depths inside the plasma membrane near the vegetal pole of immobilized eggs. Focusing upward through the vegetal pole,

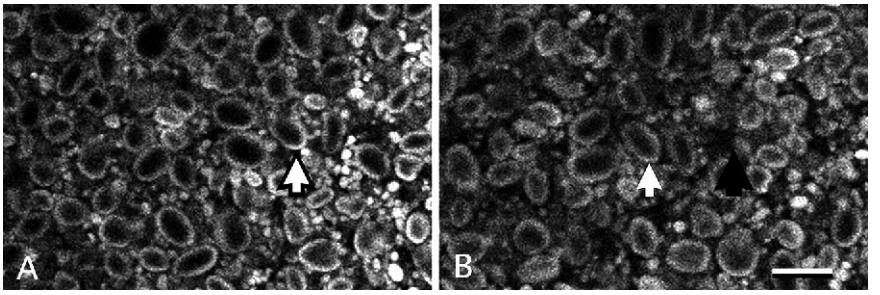

Fig. 2. Single optical sections 8 μm inside the plasma membrane at the vegetal pole of a fertilized, immobilized egg, showing the initial slow displacement of Nile Red-labeled yolk platelets between (A) 0.27 NT and (B) 0.45 NT. Yolk platelets have traveled an average of 18 μm in the 14.3 minute time interval between the images; the black arrow indicates the earlier position and the white arrow the later position, of one representative yolk platelet. Bar, 12 μm.

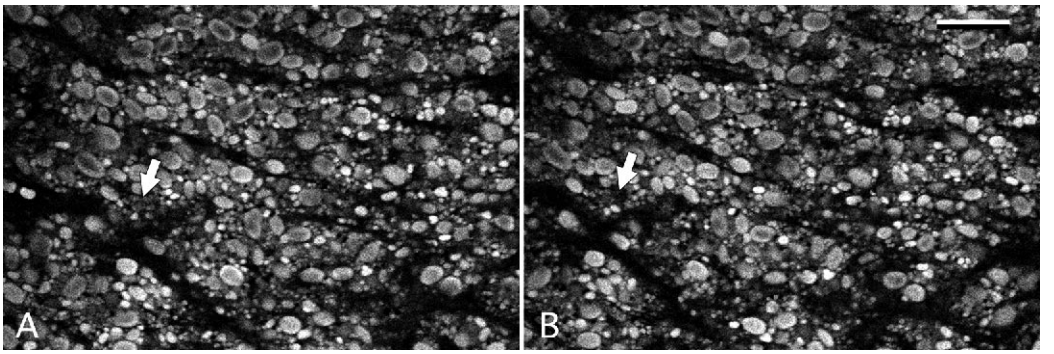

Fig. 3. Single optical sections of the region shown in Fig. 2, but at a later time. These images show rapid yolk platelet movement between (A) 0.72 NT and (B) 0.77 NT. Platelets have traveled an average of 23.5 μm in 3.1 minutes. Microtubule bundles of the parallel array can be seen as dark channels among the brightly stained yolk platelets. The microtubules bundles, which in effect are negatively stained, form distinctive patterns (such as the 'X' seen here) that can be followed through consecutive images. Specific platelets appear to be consistently associated with specific sites on the bundles, confirming that the inner cytoplasm and the parallel array move together during rotation. Bar, 30 μm.

we began our measurements where yolk platelet movements could first be detected (approximately 4-5 μm inside the plasma membrane, as shown in the optical section perpendicular to the coverslip in Fig. 5), then we continued to take measurements at increasing depths until fluorescent platelets could no longer be detected (approximately 14-15 μm inside the plasma membrane).

In one egg for which we obtained extensive data, we found that the average velocity of small to medium-sized yolk platelets (≤5 μm diameter) in the most peripheral portion of the moving yolk mass (that region about 4 μm from the egg surface) was 4.1±0.5 μm/minute, while those approximately 6 μm from the cell surface moved at an average velocity of 8.1±0.8 μm/minute. (The deviation reported for each of these figures represents the variability among measurements obtained from different yolk platelets in the same egg.) Movement near the interface between the cortex and the cytoplasmic core (at a depth of about 4 μm) was quite turbulent, with stationary organelles being jostled by those moving past them. Some smaller organelles in this interface zone exhibited sporadic movements, with short bursts interrupted by quiescent periods. At greater depths (8-14 μm inside the plasma membrane), medium- to large-sized yolk platelets (>5 μm diameter) were plentiful and tended to move more smoothly than the small yolk platelets at shallower depths, so we used them for all distance measurements at depths greater than 6 μm. In a zone approximately 8 μm deep, yolk platelets moved at a peak velocity (during the translocation phase) averaging 10.7±0.2 μm/minute. Yolk platelets deeper than 8 μm moved with an average velocity which was not significantly different from that seen at 8 μm (Fig. 6).

Analyses performed with other eggs, both fertilized and electrically activated, showed a similar increase of velocity with depth. Velocities in other fertilized eggs (n=5) varied from 5.0±1.0 μm/minute at a depth of 4 μm to 10.5±1.0 μm/minute at a depth of 8 μm. (The deviation reported for each of these figures represents the variability among means obtained from different eggs.) In activated eggs (n=3), we found that velocity varied from 5.0±1.0 μm/minute at a depth of 4 μm to 8.5±1.0 μm/minute at a depth of 8 μm, suggesting that variation of velocity with depth may be slightly less pronounced in activated eggs than in fertilized eggs.

To verify that the differences that we observed at various depths were not optical artifacts produced by the apparatus, we examined several fixed eggs as described in Materials and Methods. We found that distance measurements made at each depth in these controls were identical to within less than 1%,

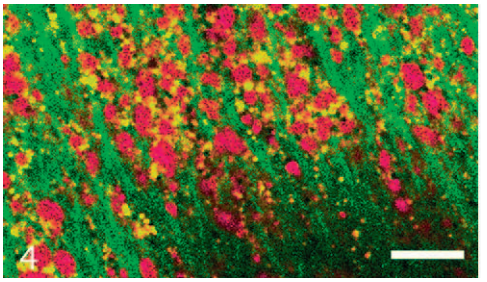

Fig. 4. Single optical section of the same region (8 μm inside the plasma membrane at the vegetal pole) in a fertilized, immobilized egg which was both stained with Nile Red and injected with fluorescein-labeled tubulin. The channels between the Nile Red-stained yolk platelets (red) are filled with fluorescein-labeled microtubules (green), confirming that the channels are negatively stained images of microtubule bundles. Optical sections were made at the rhodamine and fluorescein wavelengths simultaneously, then superimposed by computer. Bar, 50 μm.

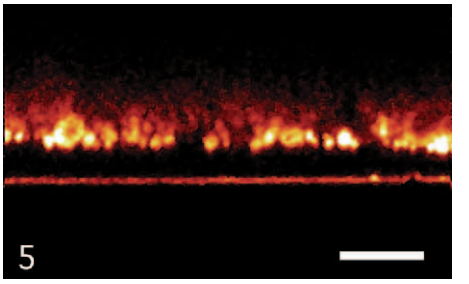

Fig. 5. Optical section perpendicular to the plasma membrane (i.e., parallel to the animal-vegetal axis) at the vegetal pole of a fertilized, immobilized egg during cortical rotation. The inner cytoplasm (indicated here by brightly stained yolk platelets) is separated from the plasma membrane by a region 4-5 μm thick which is devoid of yolk platelets. The bright red line at the bottom is the coverslip, which was coated with poly-L-lysine to insure firm adhesion of the egg surface. Bar, 20 μm.

Depth from PM (μm)	Displacement (μm)	Ave. Velocity (μm/min)
14	524	10.6 ± 0.2
12	529	10.7 ± 0.2
8	526	10.7 ± 0.8
6	398	8.1 ± 0.8
4	204	4.1 ± 0.5
0	0	0.0 ± 0.0

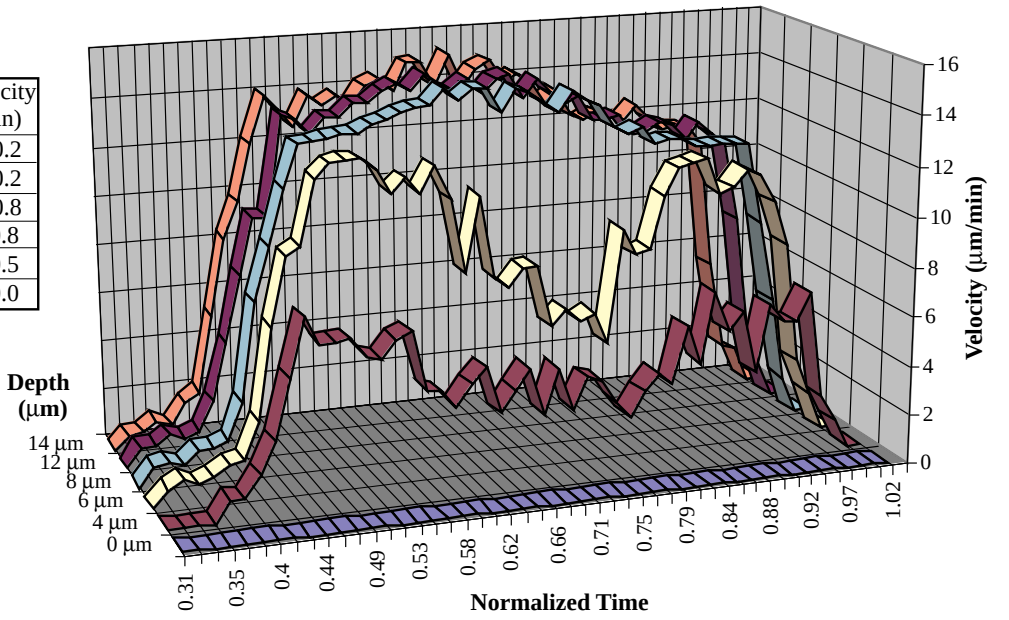

Fig. 6. Velocity of yolk platelets at five different depths inside the plasma membrane (PM) at the vegetal pole of a fertilized, immobilized egg during cortical rotation. No yolk platelets were detected in the region 0-4 μm inside the PM and confocal images deeper than 14 μm were too faint to be analyzed. In this egg, the velocity of yolk platelets during the translocation period increases with depth from 4 to 8 μm, averaging 4.1±0.5 μm/minute at a depth of 4 μm, 8.1±0.8 μm/minute at 6 μm and 10.7±0.2 μm/minute at 8 μm. (The deviation reported for each of these figures represents the variability among measurements obtained from different yolk platelets.)

indicating that the velocity differences that we observed for yolk platelets at various depths in immobilized live eggs were real.

We considered the possibility that the differences we observed were due to movements of yolk platelets along microtubules in the parallel array, rather than movements of the microtubules themselves. If yolk platelets nearest the cortex were moving toward the plus ends of microtubules, then their apparent velocity would be slower than that of the microtubules to which they were attached. In that case, even if all layers in the parallel array were moving at the same velocity relative to the cortex, those nearest the cortex would appear to be moving more slowly. To determine whether this was the case, we repeated our distance measurements in one Nile Red-stained egg by using distinctive features of the channel pattern instead of yolk platelets and found a similar velocity-depth profile. We also examined the parallel array over time at several depths in three other eggs injected with rhodamine-labeled tubulin (similar to the egg shown in Fig. 8) and found that microtubules at a depth of 4 μm moved an average of 36% of the velocity of those at 8 μm, while those at 6 μm averaged 63% of the velocity at 8 μm. Finally, we injected caged fluorescein-labeled tubulin (a gift of Tim Mitchison) into four eggs at 0.3 NT then photoactivated a 50 μm-diameter spot. In all four eggs, we observed a lengthening of the fluorescent zone with time in the direction of movement, suggesting sliding of microtubules relative to each other. Analysis of optical sections of this zone in one of the eggs showed that microtubules at a depth of 4 μm moved at approximately 49% of the velocity of microtubules at a depth of 8 μm, while those at 6 μm moved at approximately 80% of the velocity at 8 μm. All three of these methods confirmed that the velocity of microtubules as well as yolk platelets increases with depth from 4 to 8 μm.

Formation of the microtubule array

In fixed eggs, previous investigators have found a disordered mesh of microtubules in the vegetal subcortex as early as 0.35 NT (Schroeder and Gard, 1992), but well-formed parallel arrays have not been observed until approximately 0.45-0.50 NT (Elinson and Rowning, 1988; Schroeder and Gard, 1992). We stained living eggs with Nile Red to monitor their rotation movements, then rapidly fixed them and processed them for immunofluorescence (Gard, 1993; Gard and Kropf, 1993) to visualize their microtubules. Using this approach, we similarly found that early rotation movements (before 0.50 NT) were accompanied only by isolated, disorganized microtubules in the vegetal subcortex and that well-organized parallel arrays appeared only after 0.50 NT (Wells, 1994).

In living eggs, channels indicating bundled microtubules are first observed between 0.50 and 0.55 NT (Fig. 3). To determine the time course of microtubule array formation in living eggs, we monitored microtubule polymerization in eggs injected with rhodamine-labeled tubulin, collecting serial optical sections starting as early as 0.20 NT and using low intensity laser power (3%) with two minute intervals between each series to reduce photobleaching. We were not able to detect rhodamine-labeled microtubules until well after the onset of yolk platelet movements in the initiation phase of rotation (Fig. 1), though it is possible that some undetected microtubules were present earlier. We first detected short segments of labeled microtubules at approximately 0.40 NT (Fig. 7A). These segments gradually increased in length and density, and eventually attained the parallel orientation commonly associated with rotation (Fig. 7F-H). Optical sections collected at depths 1 μm apart at 0.65 NT revealed that the microtubule array near the vegetal pole during the translocation phase of rotation consists of multiple layers of microtubules 4-8 μm

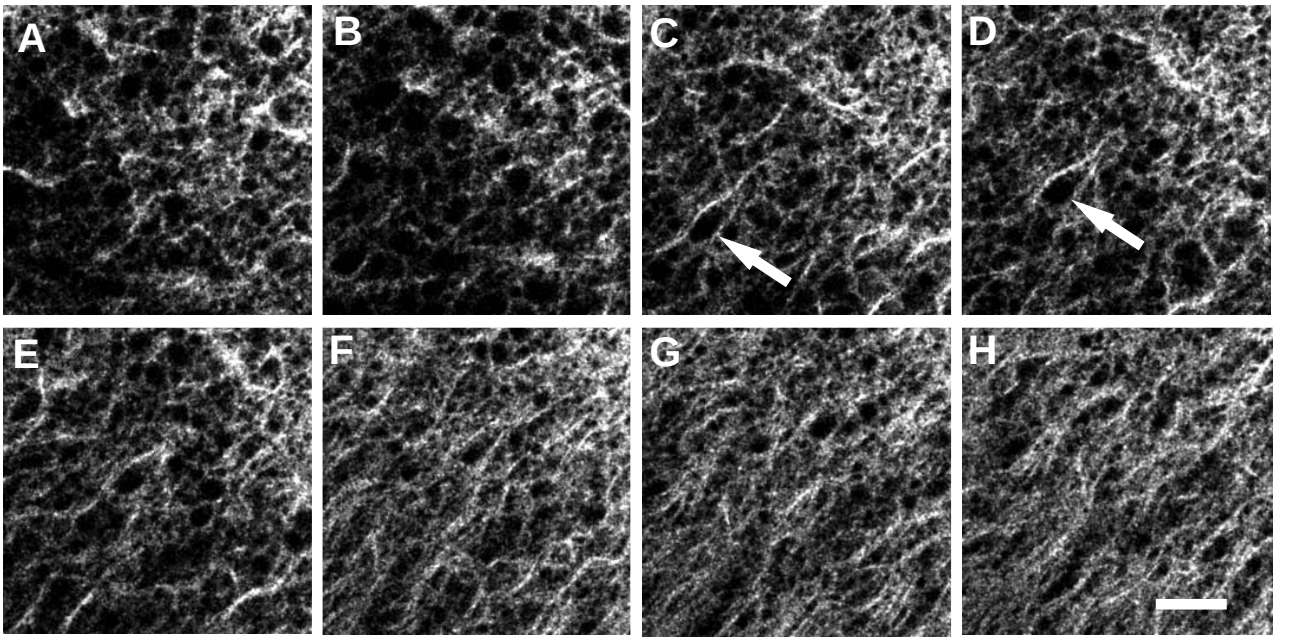

Fig. 7. Polymerization of rhodamine-labeled tubulin near the vegetal pole of a fertilized, immobilized egg, in a region 4-6 μm inside the plasma membrane. Short segments of microtubules are first detected at approximately 0.40 NT (A). Microtubules increase in length and density until 0.54 NT (H). Displacement of yolk platelets in the direction of rotation (movement of black circles from lower left to upper right of each image) can also be seen in these sections (arrows in C and D). Each image represents a single optical section. Normalized times are: A, 0.40; B, 0.42; C, 0.44; D, 0.46; E, 0.48; F, 0.50; G, 0.52; H, 0.54. Bar, 20 μm.

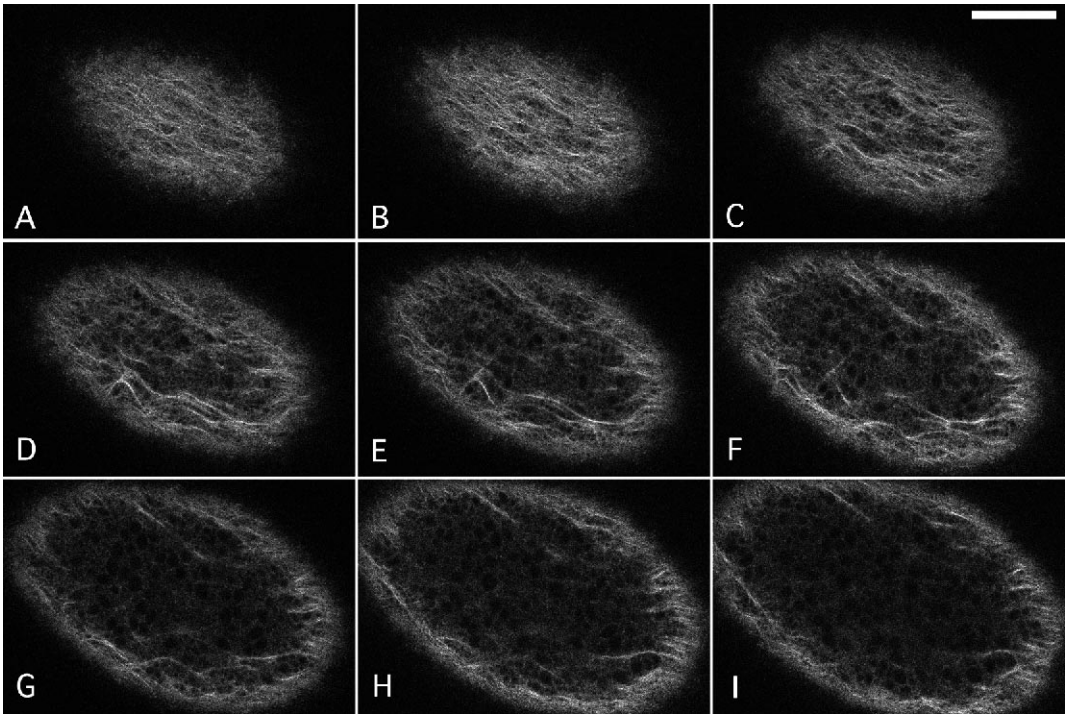

Fig. 8. Series of single optical sections near the vegetal pole of a fertilized, immobilized egg at 0.65 NT, previously injected with rhodamine-labeled tubulin. The first image (A) shows microtubules approximately 4 μm inside the plasma membrane; each successive image is 1 μm deeper. Due to the spherical shape of the egg, the microtubules visible at the periphery of the deepest sections actually lie at shallower depths. These images show that the parallel array is densest between 4 and 6 μm (A-C), and becomes less dense with depth until it is no longer detectable at depths greater than 8 μm (H-I). Bar, 100 μm.

from the egg surface (Fig. 8). In deeper sections (8-10 μm from the surface), labeled microtubules were seen only at the periphery (i.e., closer to the surface). We could not detect any labeled microtubule bundles deeper than 8 μm in the vegetal pole region of the egg. Our finding does not conflict with earlier reports of radially oriented microtubule networks at this depth (Houliston and Elinson, 1991b; Schroeder and Gard, 1992), since we looked only for microtubules parallel to the vegetal surface.

When the optical sections are played back rapidly, as a movie, the dynamic nature of the microtubules becomes quite apparent. Even after a well-developed parallel array has

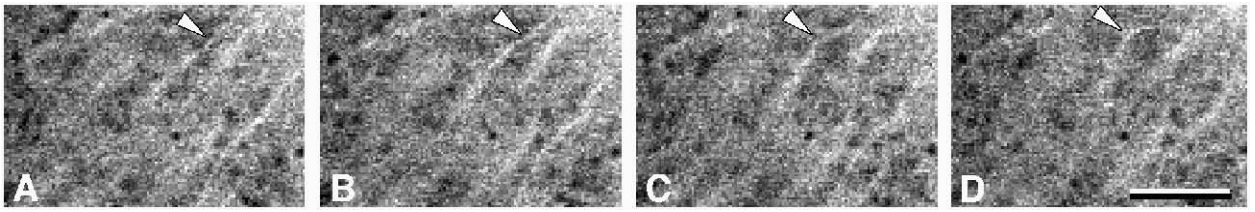

Fig. 9. Microtubule dynamics during cortical rotation. Optical sections collected very rapidly show lateral movements of microtubule bundles in the parallel array of a fertilized, immobilized egg injected with rhodamine-labeled tubulin. The arrowhead in each frame points to a segment of a microtubule bundle, which undergoes a wave-like lateral displacement of approximately 2 μm in an 18 second time interval. The black dots are pigment granules (≈0.25 μm diameter). Bar, 3 μm.

formed, the microtubules appear to be oscillating along much of their length. In many places, the microtubules appear to be 'tethered,' perhaps to organelles in the cytoplasmic core, while other segments of microtubules appear to be unattached and waving back and forth. Fig. 9 shows one of these regions over an 18-second time period as it is displaced approximately 2 μm. Such waving might be due to forces being exerted by motor molecules.

DISCUSSION

Previous work on cortical rotation in frog eggs has shown that a parallel array of microtubules just inside the vegetal cortex is probably involved in producing the necessary force. Since most of these microtubules are oriented with their plus ends facing the direction of cortical movement and since the parallel array moves with the cytoplasmic core, it has been suggested that plus end-directed motor molecules attached to the inner face of the cortex drive rotation by moving along microtubules of the parallel array.

Using an inverted confocal laser scanning microscope, we obtained a detailed picture of organelle and microtubule movements in the subcortical region near the vegetal pole of living *Xenopus* eggs undergoing cortical rotation. Our data show that (1) yolk platelet movement begins before any detectable parallel array appears at the vegetal pole, (2) the parallel array of microtubules occupies a zone approximately 4-8 μm deep inside the plasma membrane and yolk platelets in this zone move with the microtubules during cortical rotation and (3) the velocity of microtubules and yolk platelets (relative to the cortex) increases with depth from 4 μm to at least 8 μm. These data suggest that the cortical motor molecule model of force generation needs modification.

First, the movement of yolk platelets before the appearance of the parallel array suggests that something else may be producing the initial movement, which may then help to orient the parallel array. This would be consistent with the observation by Vincent and his co-workers that last-minute changes can be produced in the direction of rotation by egg inclination or compression, as well as with their conclusion that the movement-generating machinery probably "aligns itself in the direction of movement *as movement takes place*" (Vincent et al., 1987). It would also be consistent with observations that the parallel array appears to form during the initial movement rather than beforehand (Elinson and Rowning, 1988) and that a brief 90° tilt off-axis before the start of rotation can determine the orientation of the parallel array (Ziskind and Elinson, 1990).

Since movement in the initiation phase precedes the appearance of parallel microtubules at the vegetal pole, where is the force generated? Elinson and Rowning (1988) suggested that isolated single microtubules in the vegetal pole region (in conjunction with cortical motor molecules) might participate in an "autocatalytic interaction between movement and alignment." Although we did not detect such microtubules, it is nevertheless possible that they were present but that our injected tubulin did not diffuse fast enough to be incorporated in them. Alternatively, it is possible that rotation is initiated by parallel microtubules elsewhere in the subcortex; for example, astral microtubules have been found bending and running parallel to the animal hemisphere cortex as early as 0.25 (Schroeder and Gard, 1992). Yet another possibility is that rotation is initiated by a cortical actin-based mechanism. Cytochalasin B inhibits rotation if injected in high concentrations before 0.4 NT and DNAse (which depolymerizes already formed microfilaments) also inhibits rotation to varying degrees (Vincent, 1986). Vincent considered the evidence consistent with the idea that a microfilament system assembles before 0.45 NT which is used later for rotation movements.

Alternatively, cytoplasmic movements might begin deeper in the egg. Danilchik and his colleagues have reported swirling patterns in the animal hemisphere cytoplasm of fertilized *Xenopus* eggs during the rotation period (Danilchik and Denegre, 1991). By tilting eggs during the first cell cycle and by irradiating eggs vegetally with ultraviolet light (which blocks cortical rotation), they were able to show that the sperm aster not only causes the swirling but also affects yolk mass movements (Brown et al., 1993; Denegre and Danilchik, 1993). Of course, cortical rotation can occur even in the absence of a sperm aster; but deep, radially organized microtubule arrays have been found in activated and enucleated eggs and oocytes, as well as in isolated vegetal fragments (Houliston and Elinson, 1991b; Wells, 1994). Thus it is possible that the small cytoplasmic movements that initiate rotation near the cortex originate deeper in the egg.

Our second observation, that organelle movements and the parallel array were not detected at depths shallower than 4 μm, suggests that the cortex (functionally defined as the layer that moves with the plasma membrane rather than the inner cytoplasmic core) is thicker than the 1-3 μm reported previously (Grey et al., 1974; Gall et al., 1983; Houliston and Elinson, 1991a). Perhaps the discrepancy can be attributed to shrinkage due to the fixation techniques used in earlier studies. Alterna-

tively, or in addition, the discrepancy might be explained by the difference in resolution between standard epifluorescence microscopy and laser scanning confocal microscopy (Wilson, 1990).

Our third observation, that the velocity of microtubules and yolk platelets increases with depth from 4 to 8 μm, is difficult to reconcile with a model of force generation that relies on cortical motor molecules moving along a single layer of microtubules attached to the cytoplasmic core. In general, acceleration (and thus velocity) is greatest at the point where force is applied. Apparent exceptions to this rule (e.g., the increase of velocity with distance from the center of a centrifuge) require that force be rigidly transmitted from the point of application (e.g., by the rotor arms). Therefore, if force is applied only at the interface between cortex and cytoplasmic core (approximately 4-5 μm inside the plasma membrane, according to our observations), then the acceleration (and hence velocity) would be maximal at this interface unless the force were somehow being transmitted deeper.

It is conceivable that this is the case, with force generated primarily by motor molecules attached to the inner face of the cortex, which act on a few precocious, undetected microtubules that are anchored to the cytoplasmic core at least 4 μm deeper. Force generated at the inner face of the cortex could thereby be transmitted directly to the inner cytoplasm, causing it to move faster than the region nearest the cortex. This model, however, must assume that relatively few motor molecules and microtubules produce and transmit the force to move the massive cytoplasmic core.

It seems more likely that motor molecules interact with microtubules throughout the parallel array and not just at its interface with the cortex. In other words, motor molecules attached to the cortex might impart some velocity to microtubules in contact with the interface; motor molecules attached to this outer layer of microtubules might then impart additional velocity to the next deeper layer of microtubules; a similar process might then impart additional velocity to even deeper microtubules and so on. In this model, force could be generated by plus end-directed motor molecules throughout the observed 4-5 μm thickness of the parallel array, with the result that the deepest microtubules (and associated organelles of the cytoplasmic core) would move faster than those nearest the cortex.

The layered movement implied by this model may be similar to the sliding of axonemal microtubules in cilia and eukaryotic flagella. In those structures, adjacent microtubules slide past each other in a polarized fashion: motor molecules attached to microtubule N push microtubule N+1 in a plus direction, while motor molecules attached to microtubule N+1 push microtubule N+2 in a plus direction and so on (Holwill and Satir, 1990). Although dynein causes microtubule sliding in cilia and flagella (Satir, 1968; Summers and Gibbons, 1971), kinesin can also produce sliding between microtubules in vitro (Urrutia et al., 1991). It would not be surprising to find a similar sliding mechanism at work in the parallel array of rotating frog eggs. Microtubules in the parallel array are not as closely apposed to each other at all points as the microtubules in cilia and flagella, but the former also move past each other much more slowly than the latter: sliding velocities in flagella are of the order of μm/second (Smith and Sale, 1992), while the relative velocity of adjacent layers in the parallel array is of the order of μm/minute (Fig. 6). One reason for the difference might be that sliding between microtubules in the parallel array is mediated by motor molecule-bearing organelles.

It is not clear where the microtubules in the cortical array originate. There is evidence that many of them extend outward from the sperm aster (or activation aster) and bend as they reach the cortex (Schroeder and Gard, 1992). There is also evidence that some microtubules may originate in the subcortical region (Rowning, 1993). Our data do not distinguish between these two populations of microtubules. The differential sliding that we observed may involve only one of them, or may involve the movement of one population relative to the other.

A layered movement mechanism could account for the velocity gradient that we observed in immobilized eggs. Normally, however, the egg is free-floating (i.e., non-immobilized), so that the cytoplasmic core remains stationary (with gravity continually orienting the heavier yolk downwards) while the cortex rotates. If the layered movement model is correct, then the velocity (as measured by an observer outside the egg) would presumably be a minimum next to the stationary core and would increase outward toward the cortex, resulting in a gradient that is the reverse of what we observed. Alternatively, it is possible that the sort of velocity gradient that we observed exists only in immobilized eggs, resulting from the load imposed by the heavy cytoplasmic core. We did not examine non-immobilized eggs, since even slight movements of the specimen make it impossible to obtain good resolution with a laser scanning confocal microscope.

In any case, the cortical motor molecule hypothesis appears to need revision in two respects. First, rotation movements prior to the appearance of a detectable parallel array suggest that the array may be oriented by cytoplasmic movements that precede its formation. These may be due to a few precocious, undetected microtubules near the vegetal cortex, to microtubules in the equatorial or animal cortex, or to deeper cytoplasmic movements such as those reported by Danilchik and his colleagues. Second, the increase of velocity with depth suggests that not all of the force is being applied in a single plane at the interface between the cortex and the cytoplasmic core. It seems most likely that the observed velocity gradient is due to layered movement produced by motor molecules attached to microtubules throughout the entire 4-5 μm-thick parallel array.

The authors gratefully acknowledge valuable conversations with Kenneth H. Downing, David J. DeRosier and Steven W. Moore, and valuable technical help from Frank Lie of Leica. This work was supported, in part, by NIH Grant GM19363 to J. C. Gerhart.

REFERENCES

Ancel, P. and Vintemberger, P. (1948). *Recherches sur le Déterminisme de la Symétrie Bilatérale dans l'Oeuf des Amphibiens*, Laboratoire d'Evolution des Êtres Organisés, Paris.

Black, S. D. and Gerhart, J. C. (1985). Experimental control of the site of embryonic axis formation in *Xenopus laevis* eggs centrifuged before first cleavage. *Dev. Biol.* **108**, 310-324.

Brown, E. E., Denegre, J. M. and Danilchik, M. V. (1993). Deep cytoplasmic rearrangements in ventralized *Xenopus* embryos. *Dev. Biol.* **160**, 157-164.

Danilchik, M. V. and Denegre, J. M. (1991). Deep cytoplasmic rearrangements during early development in *Xenopus laevis*. *Development* **111**, 845-856.

Denegre, J. M. and Danilchik, M. V. (1993). Deep cytoplasmic

rearrangements in axis-respecified *Xenopus* embryos. *Dev. Biol.* **160**, 148-156.

Elinson, R. P. (1975). Site of sperm entry and a cortical contraction associated with egg activation in the frog *Rana pipiens*. *Dev. Biol.* **47**, 257-268.

Elinson, R. P. and Palecek, J. (1993). Independence of two microtubule systems in fertlized frog eggs: the sperm aster and the vegetal parallel array. *Roux's Arch. Dev. Biol.* **202**, 224-232.

Elinson, R. P. and Rowning, B. (1988). A transient array of parallel microtubules in frog eggs: potential tracks for a cytoplasmic rotation that specifies the dorso-ventral axis. *Dev. Biol.* **128**, 185-197.

Gall, L., Picheral, B. and Gounon, P. (1983). Cytochemical evidence for the presence of intermediate filaments and microfilaments in the egg of *Xenopus laevis*. *Biologie Cellulaire* **47**, 331-341.

Gard, D. L. (1993). Confocal immunofluorescence microscopy of microtubules in amphibian oocytes and eggs. *Methods in Cell Biology* **38**, 241-264.

Gard, D. L. and Kropf, D. L. (1993). Confocal immunofluorescence microscopy of microtubules in oocytes, eggs, and embryos of algae and amphibians. *Methods in Cell Biology* **37**, 147-169.

Gerhart, J., Danilchik, M., Roberts, J., Rowning, B. and Vincent, J.-P. (1986). Primary and secondary polarity of the amphibian oocyte and egg. *Symposia of the Society for Developmental Biology* **44**, 305-319.

Gerhart, J. C., Ubbels, G., Black, S., Hara, K. and Kirschner, M. (1981). A reinvestigation of the role of the grey crescent in axis formation in *Xenopus laevis*. *Nature* **292**, 511-516.

Greenspan, P., Mayer, E. P. and Fowler, S. D. (1985). Nile red: a selective fluorescent stain for intracellular lipid droplets. *J. Cell Biol.* **100**, 965-973.

Grey, R. D., Wolf, D. P. and Hedrick, J. L. (1974). Formation and structure of the fertilization envelope in *Xenopus laevis*. *Dev. Biol.* **36**, 44-61.

Holwill, M. E. J. and Satir, P. (1990). A physical model of microtubule sliding in ciliary axonemes. *Biophys. J.* **58**, 905-917.

Houliston, E. (1994). Microtubule translocation and polymerisation during cortical rotation in *Xenopus* eggs. *Development* **120**, 1213-1220.

Houliston, E. and Elinson, R. P. (1991a). Evidence for the involvement of microtubules, ER, and kinesin in the cortical rotation of fertilized frog eggs. *J. Cell Biol.* **114**, 1017-1028.

Houliston, E. and Elinson, R. P. (1991b). Patterns of microtubule polymerisation relating to cortical rotation in *Xenopus laevis* eggs. *Development* **112**, 107-117.

Houliston, E., Le Guellec, R., Kress, M., Phillipe, M. and Le Guellec, K. (1994). The kinesin-related protein Eg5 associates with both interphase and spindle microtubules during *Xenopus* early development. *Dev. Biol.* **164**, 147-159.

Kirschner, M., Gerhart, J., Hara, K. and Ubbels, G. A. (1980). Initiation of the cell cycle and establishment of bilateral symmetry in *Xenopus* eggs. *Symposia of the Society for Developmental Biology* **38**, 187-215.

Manes, M. E., Elinson, R. P. and Barbieri, F. D. (1978). Formation of the amphibian egg gray crescent: effects of colchicine and cytochalasin B. *Roux's Arch. Dev. Biol.* **185**, 99-104.

Rowning, B. (1993). Microtubule-mediated cortical rotation in the first cell cycle *Xenopus* egg. Ph.D. Thesis, University of California at Berkeley.

Sardet, C., Speksnijder, J., Inoue, S. and Jaffe, L. (1989). Fertilization and ooplasmic movements in the ascidian egg. *Development* **105**, 237-249.

Satir, P. (1968). Studies on cilia: III. Further studies on the cilium tip and a 'sliding filament' model of ciliary motility. *J. Cell Biol.* **39**, 77-94.

Sawada, T. and Schatten, G. (1989). Effects of cytoskeletal inhibitors on ooplasmic segregation and microtubule organization during fertilization and early development in the ascidian *Molgula occidentalis*. *Dev. Biol.* **132**, 331-342.

Sawin, K. E. and Mitchison, T. J. (1991). Poleward microtubule flux in mitotic spindles assembled *in vitro*. *J. Cell Biol.* **112**, 941-954.

Schroeder, M. M. and Gard, D. L. (1992). Organization and regulation of cortical microtubules during the first cell cycle of *Xenopus* eggs. *Development* **114**, 699-709.

Smith, E. F. and Sale, W. S. (1992). Regulation of dynein-driven microtubule sliding by the radial spokes in flagella. *Science* **257**, 1557-1559.

Summers, K. E. and Gibbons, I. R. (1971). Adenosine triphosphate-induced sliding of tubules in trypsin-treated flagella of sea-urchin sperm. *Proc. Natn Acad.Sci.USA* **68**, 3092-3096.

Theurkauf, W. E. (1994). Premature microtubule-dependent cytoplasmic streaming in *cappuccino* and *spire* mutant oocytes. *Science* **265**, 2093-2096.

Theurkauf, W. E., Alberts, B. M., Jan, Y. N. and Jongens, T. A. (1993). A central role for microtubules in the differentiation of *Drosophila* oocytes. *Development* **118**, 1169-1180.

Ubbels, G. A., Hara, K., Koster, C. H. and Kirschner, M. W. (1983). Evidence for a functional role of the cytoskeleton in determination of the dorsoventral axis in *Xenopus laevis* eggs. *J. Embryol. Exp. Morph.* **77**, 15-37.

Urrutia, R., McNiven, M. A., Albanesi, J. P., Murphy, D. B. and Kachar, B. (1991). Purified kinesin promotes vesicle motility and induces active sliding between microtubules *in vitro*. *Proc. Natn Acad. Sc. USA* **88**, 6701-6705.

Vincent, J.-P. (1986). The first cell cycle reorganization at the periphery of fertilized *Xenopus* eggs. Ph.D. Thesis, University of California at Berkeley.

Vincent, J.-P., Oster, G. F. and Gerhart, J. C. (1986). Kinematics of gray crescent formation in *Xenopus* eggs: The displacement of subcortical cytoplasm relative to the egg surface. *Dev. Biol.* **113**, 484-500.

Vincent, J.-P., Scharf, S. R. and Gerhart, J. C. (1987). Subcortical rotation in *Xenopus* eggs: A preliminary study of its mechanochemical basis. *Cell Motility and the Cytoskeleton* **8**, 143-154.

Wells, J. C. (1994). A confocal microscopy study of microtubule arrays involved in cortical rotation during the first cell cycle of *Xenopus* embryos. Ph.D. Thesis, University of California at Berkeley.

Wilson, T. (1990). *Confocal Microscopy*. London: Academic Press.

Zisckind, N. and Elinson, R. P. (1990). Gravity and microtubules in dorsoventral polarization of the *Xenopus* egg. *Development, Growth & Differentiation* **32**, 575-581.

(Accepted 17 January 1996)